J Physiol 589.24 (2011) pp 6093–6104

The Journal of Physiology

Biophysical properties of slow potassium channels in human embryonic stem cell derived cardiomyocytes implicate subunit stoichiometry

Kai Wang[1], Cecile Terrenoire[1], Kevin J. Sampson[1], Vivek Iyer[2], Jeremiah D. Osteen[1], Jonathan Lu[2], Gordon Keller[3], Darrell N. Kotton[4] and Robert S. Kass[1]

Departments of [1] Pharmacology and [2] Medicine, College of Physicians and Surgeons, Columbia University Medical Center, New York, NY, USA
[3] McEwen Centre for Regenerative Medicine, University Health Network, Toronto, Canada
[4] The Pulmonary Center, Boston University School of Medicine, Boston, MA, USA

Non-technical summary The human heart is a pump that works only when its internal electrical system coordinates both its filling and its capacity to eject blood. This critical electrical timing is coordinated by many different ion channels, and this study looks at the one known as I_{Ks}. Mutations in its α subunit, KCNQ1, constitute the majority of cases of the disorder long QT syndrome (LQT-1). Here we have examined properties of human cardiac cells during very early stages of development and found evidence for the manner in which the subunits of I_{Ks} assemble; our data suggest that this assembly may be flexible and may change during development and/or disease.

Abstract Human embryonic stem cells (hESCs) are an important cellular model for studying ion channel function in the context of a human cardiac cell and will provide a wealth of information about both heritable arrhythmias and acquired electrophysiological disorders. However, detailed electrophysiological characterization of the important cardiac ion channels has been so far overlooked. Because mutations in the gene for the I_{Ks} α subunit, KCNQ1, constitute the majority of long QT syndrome (LQT-1) cases, we have carried out a detailed biophysical analysis of this channel expressed in hESCs to establish baseline I_{Ks} channel biophysical properties in cardiac myocytes derived from hESCs (hESC-CMs). I_{Ks} channels are heteromultimeric proteins consisting of four identical α-subunits (KCNQ1) assembled with auxiliary β-subunits (KCNE1). We found that the half-maximal I_{Ks} activation voltage in hESC-CMs and in myocytes derived from human induced pluripotent stems cells (hiPSC-CMs) falls between that of KCNQ1 channels expressed alone and with full complement of KCNE1, the major KCNE subunit expressed in hESC-CMs as shown by qPCR analysis. Overexpression of KCNE1 by transfection of hESC-CMs markedly shifted and slowed native I_{Ks} activation implying assembly of additional KCNE1 subunits with endogenous channels. Our results in hESC-CMs, which indicate an I_{Ks} subunit stoichiometry that can be altered by variable KCNE1 expression, suggest the possibility for variable I_{Ks} function in the developing heart, in different tissues in the heart, and in disease. This establishes a new baseline for I_{Ks} channel properties in myocytes derived from pluripotent stem cells and will guide future studies in patient-specific hiPSCs.

(Resubmitted 18 September 2011; accepted 22 October 2011; first published online 24 October 2011)
Corresponding author R. S. Kass: Department of Pharmacology, Columbia University Medical Center, 630 W. 168th Street, PH 3-718, New York, NY 10032, USA. Email: rsk20@columbia.edu

K. Wang and C. Terrenoire shared equally in this work.

DOI: 10.1113/jphysiol.2011.220863

Abbreviations CTX, charybdotoxin; CTX-KCNQ1, charybdotoxin sensitive KCNQ1 channel; FAF, familial atrial fibrillation; hESC, human embryonic stem cell; hiPSC, human induced pluripotent stem cell; hESC-CM, human embryonic stem cell derived cardiomyocyte; hiPSC-CM, human induced pluripotent stem cell derived cardiomyocyte; I_{Kr}, rapid potassium channel; I_{Ks}, slow potassium channel; LQTS, long QT syndrome; $V_{1/2}$, half-maximal activation voltage.

Introduction

I_{Ks} channels are major regulators of cardiac electrical activity (Kass & Wiegers, 1982; Terrenoire *et al.* 2005) and are formed by heteromultimers each containing four identical α-subunits (KCNQ1) assembled with auxiliary β-subunits (KCNE1). Co-assembly of KCNQ1 and KCNE1 confers distinct biophysical properties on the channels: a slowing of activation and deactivation kinetics and a large depolarizing shift in activation, critically determining the timing of their role during repolarization of the cardiac action potential (Barhanin *et al.* 1996; Sanguinetti *et al.* 1996; Schwake *et al.* 2003). Mutations in the genes for KCNQ1 and KCNE1 have been associated with long QT syndrome (LQTS) and familial atrial fibrillation (FAF) (Tsai *et al.* 2008; Lu & Kass, 2010). Human induced pluripotent stem cells (hiPSCs) were developed in addition to human embryonic stem cells (hESCs) in order to investigate the mechanistic basis of these inherited disorders and to develop patient-specific treatments (Yoshida & Yamanaka, 2010). A first step in these studies consists in determining the basic cellular electrophysiological properties of hESC derived cardiomyocytes (hESC-CMs).

The slowly activating E-4031 resistant I_{Ks} channel is a critical determinant of cellular cardiac electrical activity and mutations of either of its two principal subunits, KCNQ1 (α) or KCNE1 (β), underlie heritable arrhythmias. While mRNA for I_{Ks} channel subunits has been detected in hESC-CMs (Fu *et al.* 2010; Otsuji *et al.* 2010), the functional properties of endogenous I_{Ks} channels have not been characterized. Here we report the biophysical characterization of genotype-negative I_{Ks} channels in single hESC-CMs and hiPSC derived cardiomyocytes (hiPSC-CMs) using whole cell patch clamp recordings. The I_{Ks} channels in the hESC-CMs differ in their voltage-dependent properties from KCNQ1/KCNE1 channels in established heterologous systems including mammalian cell lines (Wang *et al.* 1998; Marx *et al.* 2002; Imredy *et al.* 2008; Chung *et al.* 2009) and are remarkably similar to those of I_{Ks} channels recorded in hiPSC-CMs. In order to determine whether hESC-CMs' background affects I_{Ks} biophysical properties, we engineered charybdotoxin-sensitive KCNQ1 channels (CTX-KCNQ1) (Chen *et al.* 2003; Morin & Kobertz, 2008) providing a means to separate expressed from endogenous current. CTX-KCNQ1 was transiently expressed in hESC-CMs in the presence or absence of KCNE1. In this manner we show that the mid-point of activation of endogenous I_{Ks} in hESC-CMs lies between KCNQ1 alone and KCNQ1/KCNE1 heteromultimers. qPCR experiments show that KCNE1 is the major KCNE subunit expressed in hESC-CMs and transfection of KCNE1 alone in hESC-CMs modifies endogenous I_{Ks} channels so as to match the expressed KCNQ1/KCNE1 channels. Our results suggest that in hESC-CMs, endogenous I_{Ks} is produced by KCNQ1 subunits assembled with KCNE1 subunits, but the subunit stoichiometry is such that it permits assembly with additional KCNE1 subunits. These data thus suggest variable α and β subunit stoichiometry in hESC-CM I_{Ks} channels that may be modulated further with changes in KCNE1 expression that occur in the developing heart or in disease.

Methods

Human fibroblast reprogramming and characterization of iPSC

The subjects who contributed to this study gave informed written consent and the experiments were conducted in accordance with the *Declaration of Helsinki*.

Dermal fibroblasts were obtained from two healthy volunteers without mutations in the major LQT-related genes (KCNQ1, KCNH2, SCN5A, KCNE1 and KCNE2) by punch biopsy. Reprogramming was performed with the hSTEMCCA-loxP lentiviral vector, encoding the four human factors, OCT4, KLF4, SOX2 and cMYC, as previously described (Somers *et al.* 2010). Briefly, 1×10^5 dermal fibroblasts were plated in Dulbecco's modified Eagle's medium (DMEM) with 10% fetal bovine serum (FBS) on a gelatin-coated 35 mm plastic tissue culture dish. The next day polybrene was added to the medium ($5\,\mu g\,ml^{-1}$) and the cells were infected with hSTEMCCA-loxP lentiviruses at a multiplicity of infection (MOI) of 1. Candidate iPSC colonies were mechanically isolated and expanded on MEF feeder cells prior to characterization by immunostaining to confirm expression of markers SSEA4, TRA1/18 and TRA1/60. Normal karyotype was confirmed by G-banding analysis. Teratoma assay was used to confirm capacity to undergo differentiation into derivatives of the three primary germ layers.

hESCs and hiPSCs maintenance and directed cardiac differentiation

hESC line hES2 from ES Cell International (Singapore) was maintained on mouse embryonic fibroblasts as

previously described (Kennedy *et al.* 2007). For both hES2 and hiPS cells, cardiac differentiation was induced by systematically staging, *in vitro*, the events that occur in a developing embryo, by exposing the hESCs and hiPSCs to cytokines using a previously reported procedure (Yang *et al.* 2008). In the present experiments, cell differentiation was, however, not followed by cell sorting to avoid the associated shear stress.

Cardiomyocyte dissociation

Beating embryoid bodies at 25–45 days post-differentiation were dissociated for 25–30 min at 37°C in the presence of collagenase II (200 units ml^{-1}, Invitrogen) and protease XIV (0.2 units ml^{-1}, Sigma-Aldrich) in a solution containing (in mmol l^{-1}): 120 NaCl, 5.4 KCl, 5 $MgSO_4$, 5 sodium pyruvate, 20 glucose, 20 taurine, 10 Hepes, pH 6.9. Isolated cells were then incubated at room temperature for 30 min in Kraft–Brühe (KB) solution containing (in mmol l^{-1}): 85 KCl, 30 K_2HPO_4, 5 MgSO4, 1 EGTA, 2 Na_2ATP, 5 sodium pyruvate, 5 creatine, 20 taurine, 20 glucose, pH 7.2. Cells were finally resuspended in DMEM supplemented with 10% FBS, 1 mmol l^{-1} sodium pyruvate and 2 mmol l^{-1} L-glutamine, and plated on 0.1% gelatin-coated 35 mm plastic Petri dishes. Isolated cardiomyocytes were identified the next day by spontaneous contraction at ∼37°C; individually marked with an object marker (Nikon); and used for recordings of endogenous I_{Ks} within 48 h after plating.

Heterologous expression

Recombinant I_{Ks} channel subunits were transiently expressed in human embryonic kidney (HEK) 293 cells and in hESC-CMs using Lipofectamine-PLUS Reagents (Lipofectamine for HEK293 cells or Lipofectamine LTX for hESC-CMs) (Invitrogen). All the genes of interest were subcloned into pcDNA3.1 vector (Invitrogen). Depending on experiments, the following DNAs were transfected: wild-type (WT) KCNQ1, KCNQ1_KCNE1 tandem multimer (Wang *et al.* 1998), charybdotoxin-sensitive KCNQ1 (CTX-KCNQ1; Chen *et al.* 2003; a kind gift from Dr William R. Kobertz University of Massachusetts Medical School, Worcester), KCNE1 (KCNQ1 and KCNE1 cDNAs were co-transfected at 1:1 ratio), KCNE4 (a kind gift from Dr Al George Jr, Department of Pharmacology, Vanderbilt University, Nashville). For transfection in hESC-CMs, cells were plated at the density of 10^4 per 35 mm Petri dish. Five hours later 0.2 μg of DNA(s) of interest was transfected according to the manufacturer's protocol overnight in the culture medium. eGFP was co-transfected with channels subunits to identify transfected cells. About 50% transfection efficiency assessed by the eGFP expression was achieved in hESC-CMs within 24 h after transfection. For both HEK293 cells and transfected hESC-CMs, patch-clamp recordings were carried out on GFP positive cells 48 h after transfection.

Quantitative real time PCR (qPCR)

Total RNA was isolated from cell culture using the Qiagen Micro RNeasy kit (Qiagen, Valencia, CA, USA) following the manufacturer's protocols. One microgram of RNA was used to generate cDNA using the SuperScript III kit (Invitrogen). Preparations of cDNA were free of genomic contamination as verified by performing a reverse-transcription step without the SuperScript III enzyme and subsequent qPCR. qPCR was performed on the LightCycler 480 Real-Time PCR System using the SYBR Green I Master (Roche) and the following amplification protocol: 5 min at 95°C, 50 cycles (15 s at 94°C – 10 s at 60°C – 10 s at 72°C). All reactions were carried out in 96-well plates. Samples were amplified in triplicate. Standard curves were generated using sample cDNA in 1:10 dilutions by plotting the cycle numbers of crossing point (cp) *versus* the common log of the relative concentrations (Supplemental Fig. S2). The corresponding PCR efficiency was calculated from the slope of the standard curve with the formula of efficiency $= 10^{(-1/\text{slope})}$. Relative quantification was done using the standard curve method with PCR efficiency correction (E-method) of the LightCycler 480 Software (Roche) (Tellmann, 2006). All samples were normalized to GAPDH expression on the same plate. Primers used were: GAPDH F: 5′-TGTTGCCATCAATGACCCCTT-3′, R: 5′-CTCCACGACGTACTCAGCG-3′; KCNQ1 F: 5′-CCCTGAAGGTGCAGCAGAA-3′, R: 5′-GCCTTCCGGATGTAGATCTTCC-3′; KCNE1 F: 5′-TGTGGCAGGAGACAGTTCAG-3′, R: 5′-GCTTCTTGGAGCGGATGTAG-3′; KCNE2 F: 5′-CAGAACAGCCTGGCTTTGGA-3′, R: 5′-TCCAGCGTCTGTGTGAAATTG-3′; KCNE3 F: 5′-ACTGAGAGCCAGTGGATTTGC-3′, R: 5′-AGGTCTCCGTTCCATTGGTAGTC-3′; KCNE4 F: 5′-AACCCTCTTGGACTGGACGAT-3′, R: 5′-AGGCTCCATTTTCAGCATTGA-3′; KCNE5 F:5′-CCCCTACCCCGCACATC-3′, R: 5′-TTGGACGTGTTGGATTCAGTTC-3′. Primers for KCNQ1 and KCNE2-5 have been published previously (Lundquist *et al.* 2005).

Single cell electrophysiology

Cells were placed on the stage of an inverted microscope (Nikon) and currents were recorded at room temperature (23–25°C) using the whole-cell configuration of the patch-clamp technique carried out with Axopatch 200B amplifiers (Axon Instruments, Union City, CA, USA). Averaged cell capacitance was: 26.5 ± 2.7 pF ($n = 28$) for HEK293 cells, 45.1 ± 6.8 pF ($n = 24$) for hESC-CMs

and 42.3 ± 6.1 pF ($n = 12$) for hiPSC-CMs. For voltage clamp experiments, we used a previously described internal recording solution (Terrenoire *et al.* 2005) and the following external solution (in mmol l^{-1}): 132 NaCl, 4.8 KCl, 2 $CaCl_2$, 1.2 $MgCl_2$, 0.05 $NiSO_4$, 10 Hepes, 5 glucose, 1 μmol l^{-1} isradipine, pH 7.4. Endogenous I_{Ks} channels were recorded in the presence of E4031 (5 μmol l^{-1}) in external recording solution in order to block the rapidly activating delayed rectifier I_{Kr}. Endogenous I_{Ks} channels were dissected pharmacologically with chromanol 293B (30 μmol l^{-1}) whereas CTX-KCNQ1 channels were isolated with CTX (70 nmol l^{-1}). Control experiments confirmed that at this concentration CTX did not affect endogenous currents (Supplemental Fig. S1). All reagents were purchased from Sigma-Aldrich (St Louis, MO, USA), unless otherwise specified. The voltage protocol and analysis for all voltage clamp experiments were as follows: cells were depolarized from −40 mV to 50 mV (in 10 mV increments) for 2 s and then repolarized to −40 mV for 2 s (holding potential was −40 mV) at a pulse frequency of 0.1 Hz. Maximum tail current amplitudes were measured during this repolarizing pulse and plotted *vs.* pre-pulse voltage (i.e. test pulse voltage). Activation curves (2 s isochronal), determined from amplitudes of deactivating current tails normalized to maximum tail current plotted *vs.* test pulse voltage, were fitted with a Boltzman equation to determine channels mid-point of activation ($V_{1/2}$). For current clamp experiments, the internal solution was the same as in voltage clamp except that potassium aspartate was replaced by KCl. External solution was (in mmol l^{-1}): 132 NaCl, 4.8 KCl, 2 $CaCl_2$, 1.2 $MgCl_2$, 10 Hepes, 5 glucose, pH 7.4. Action potentials (APs) were triggered at 1 Hz by 3 ms suprathreshold stimulations.

Computer simulation

Computational models for KCNQ1 gating (Seebohm *et al.* 2003) and KCNQ1–KCNE1 gating (Imredy *et al.* 2008) were implemented, as previously described (Sampson *et al.* 2010).

Data analysis

Patch clamp data were acquired with pCLAMP 8.2 (Axon Instruments) and analysed with Origin 7.0 (OriginLab, Northampton, MA, USA) and Clampfit 8.2 (Axon Instruments). Data are shown as means ± SEM. Statistical data analyses were assessed with Student's *t* test for simple comparisons or one-way ANOVA followed by Tukey's test for multiple comparisons: differences at $P < 0.05$ were considered as statistically significant.

Results

Action potentials in cytokine-induced differentiation of hES2 cells: enrichment in ventricular-like cellular activity

We first sequenced the Long QT genes of the hES2 line and confirmed that KCNQ1 and KCNE1 were free of any known polymorphisms or disease causing mutations.

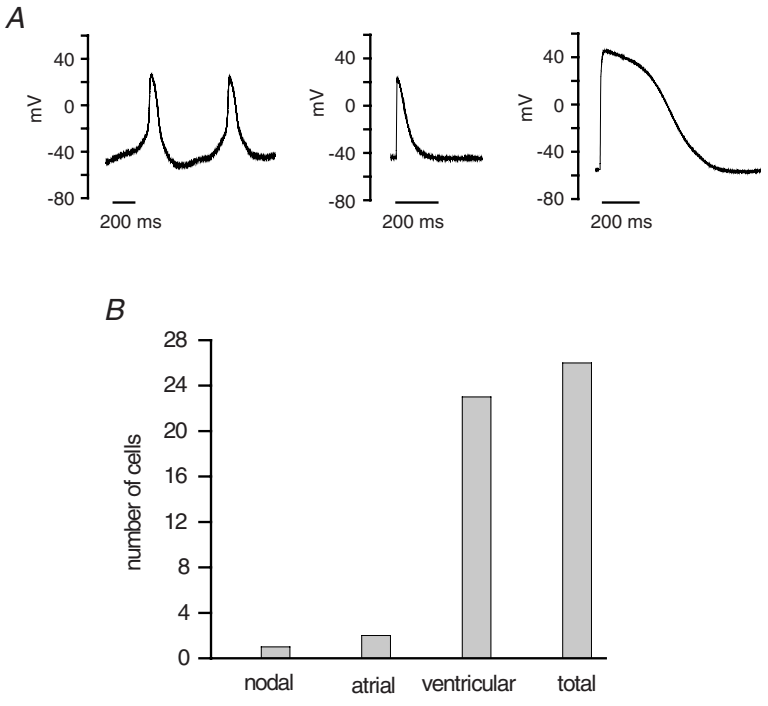

Figure 1. Action potentials phenotypes in cardiomyocytes derived from hES2 cells (hESC-CMs) by cytokine-induced differentiation
A, in a total of 26 hESC-CMs, 3 different types of action potentials (APs) were recorded: nodal-like (left panel), atrial-like (middle panel, average of 2 cells) and ventricular-like (right panel, average of 23 cells). Atrial-like and ventricular-like APs were elicited by suprathreshold stimuli at 1 Hz. All experiments were carried out at room temperature. *B*, distribution of cardiomyocytes according to their AP phenotype: out of 26 cells, one cell was nodal-like, 2 cells were atrial-like and 23 cells were ventricular-like.

Table 1. Action potential properties in cardiomyocytes derived from hES2 cells

	Overshoot (mv)	Amplitude (mV)	APD (ms)			MDP (mV)	*n* (total)
			APD_{25}	APD_{50}	APD_{90}		
Pacemaker-like	25.2	75.1	36.1	71.3	170.3	−49.9	1
Atrial-like	23.3 ± 2.5	67.9 ± 8.6	34.6 ± 11.1	50.7 ± 14.2	97.3 ± 28.5	−46.9 ± 12.5	2
Ventricular-like	47.3 ± 1.2	102.5 ± 1.7	333.1 ± 18.3	423.9 ± 22.7	513.6 ± 28.4	−62.4 ± 1.2	23

$APD_{25/50/90}$, action potential duration at 25%, 50% or 90% of maximal amplitude. MDP, maximum diastolic potential. For atrial-like and ventricular-like cells, parameters were measured on APs stimulated at 1 Hz. Data are expressed as means ± SEM.

Then we carried out current clamp experiments in single cells to characterize action potentials in single hES2 CMs. Action potentials (APs) were recorded in a total of 26 cells and were classified into three categories as reported by other groups (Mummery *et al.* 2003; Moore *et al.* 2008): (i) ventricular-like: most negative diastolic potentials, significant plateau phase and long action potential duration (APD); (ii) atrial-like: APs triangular waveform; diastolic potentials more positive and APD significantly shorter than ventricular like cells; and (iii) nodal-like APs: small amplitude, depolarized diastolic potential, and robust spontaneous activity (Fig. 1*A*, Table 1). Of the 26 cardiomyocytes we recorded, ∼90% (23 out of 26 cells) exhibited a ventricular phenotype whereas a very small number of cells were atrial-like (2 cells out of 26) and nodal-like (1 cell out of 26) (Fig. 1*B*). This clearly shows that cytokine-induced differentiation of hES2 cells produces a relatively homogeneous population of ventricular-like cardiomyocytes.

Biophysical properties of endogenous I_{Ks} in hESC-CMs

We used pharmacological dissection to identify and separate two important delayed rectifier K^+ channels that we detected under whole cell voltage clamp in these cells, I_{Kr} and I_{Ks} (Sanguinetti & Jurkiewicz, 1990), and illustrated this approach in Fig. 2. In the maintained presence of chromanol 293B (30 μmol l^{-1}), a known I_{Ks} blocker (Busch *et al.* 1996), I_{Kr} was identified as E4031 (5 μmol l^{-1})-sensitive time-dependent current (Fig. 2*A*). Typical I_{Kr} rectification properties are apparent in these current traces and on the current–voltage relationship determined by current at the end of test pulses. In the maintained presence of E-4031 (5 μmol l^{-1}), I_{Ks} was identified as chromanol 293B (30 μmol l^{-1})-sensitive time-dependent current, with kinetics and voltage-dependent activation consistent with I_{Ks} channels (Fig. 2*B*). We focused on I_{Ks} for the remainder of this study and thus included E-4031 (5 μmol l^{-1}) in all external recording solutions that follow to block I_{Kr}.

Biophysical properties of endogenous hESC-CM I_{Ks} channels: comparison with expression in hiPSC-CM and transiently transfected HEK 293 cells

Quantitative PCR (qRT-PCR) analysis of hESC-CMs revealed that the principal KCNE variant expressed in these cells is KCNE1. KCNE2, KCNE3 and KCNE5 transcripts were detectable only at very small levels, and KCNE1 transcripts are significantly greater than transcripts for the other potential I_{Ks} channel subunit, KCNE4 (Supplemental Fig. S2). Furthermore channels of only KCNQ1 and KCNE4 result in no current (Lundquist *et al.* 2005) and as such would not be observable in the hESC-CMs. We confirm that channels containing both KCNE1 and KCNE4 subunits have identical properties to KCNQ1/KCNE1 channels other than a decrease in amplitude (Grunnet *et al.* 2002) (Supplemental Fig. S3). Therefore, while KCNE4 may well be in complex with these channels, the lack of an effect on channel function allows us to focus on KCNQ1/KCNE1 channels.

I_{Ks} channels are tetrameric channels formed by co-assembly of four α (KCNQ1) subunits and auxiliary β subunits (KCNE1) (Barhanin *et al.* 1996; Sanguinetti *et al.* 1996) with subunit stoichiometry that has been reported to be variable by some groups (Wang *et al.* 1998; Nakajo *et al.* 2010) and fixed by others (Morin & Kobertz, 2008). Biophysical properties of expressed channels can be used to distinguish some aspects of subunit composition of the functioning channels. For example, it is well known that in the absence of KCNE1, KCNQ1 encodes functioning channels with rapid activation kinetics and activation voltages that are relatively negative (Fig. 3*A* and *C*) (Barhanin *et al.* 1996; Sanguinetti *et al.* 1996), and thus homomeric KCNQ1 channel activity can be distinguished from activity of heteromeric KCNQ1/KCNE1 channels expressed in the same cell line (HEK 293) both by the markedly slower activation kinetics and more positive activation voltages (Fig. 3*A* and *C*). When the KCNQ1/KCNE1 stoichiometry is fixed at a 1:1 ratio in a tandem multimer (Fig. 3*A* and *C*), both activation kinetics and voltage dependence are virtually identical to independently expressed KCNQ1 and KCNE1 with ratios of KCNE1/KCNQ1 cDNA of

1. In genotype-negative hESC-CMs and hiPSC-CMs, the biophysical properties of I_{Ks} channels are identical (Fig. 3*B* and *D*) and fall between homomeric KCNQ1 and heteromultimeric KCNQ1/KCNE1 channels with a 1:1 stoichiometry (Fig. 3*C*). As illustrated in Fig. 3*D*, the mid-point of activation ($V_{1/2}$) of endogenous I_{Ks} in hESC-CMs was 9.1 ± 1.7 mV ($n = 11$), not significantly different from the one measured in two different hiPSC lines (hiPS no. 1: $V_{1/2} = 5.1 \pm 1.4$ mV, $n = 4$; hiPS no. 2: $V_{1/2} = 10.3 \pm 2.9$ mV, $n = 8$). However, as shown in Fig. 3*C*, the mid-point of activation of endogenous I_{Ks} in hESC-CMs was between that of KCNQ1 ($V_{1/2} = -21.3 \pm 1.5$ mV, $n = 4$, $P < 0.001$) and KCNQ1+KCNE1 channels ($V_{1/2} = 29.1 \pm 1.2$ mV, $n = 9$, $P < 0.001$) as well as KCNQ1_KCNE1 tandem multimer ($V_{1/2} = 28.5 \pm 2.1$ mV, $n = 7$, N.S. compared to KCNQ1+KCNE1).

Recombinant I_{Ks} channels expressed in hESC-CMs do not reconstitute endogenous I_{Ks}

Next, in order to test whether the hESC-CMs background affects I_{Ks} biophysical properties, KCNQ1 and KCNE1 were transiently transfected in these cells. To distinguish the transfected channels from the endogenous I_{Ks} channels, we engineered KCNQ1 channels to impart a sensitivity to CTX. Consistently with a previous report (Chen *et al.* 2003), we found that CTX-sensitive channels (CTX-KCNQ1) share the same biophysical properties as wild-type (WT) channels when expressed in a heterologous system (in HEK293 cells, CTX-KCNQ1: $V_{1/2} = -26.5 \pm 4.5$ mV, $n = 4$, and CTX-KCNQ1/KCNE1: $V_{1/2} = 26.8 \pm 2.1$ mV, $n = 4$; N.S. compared to corresponding WT channels in HEK293 cells shown in Fig. 3*C*).

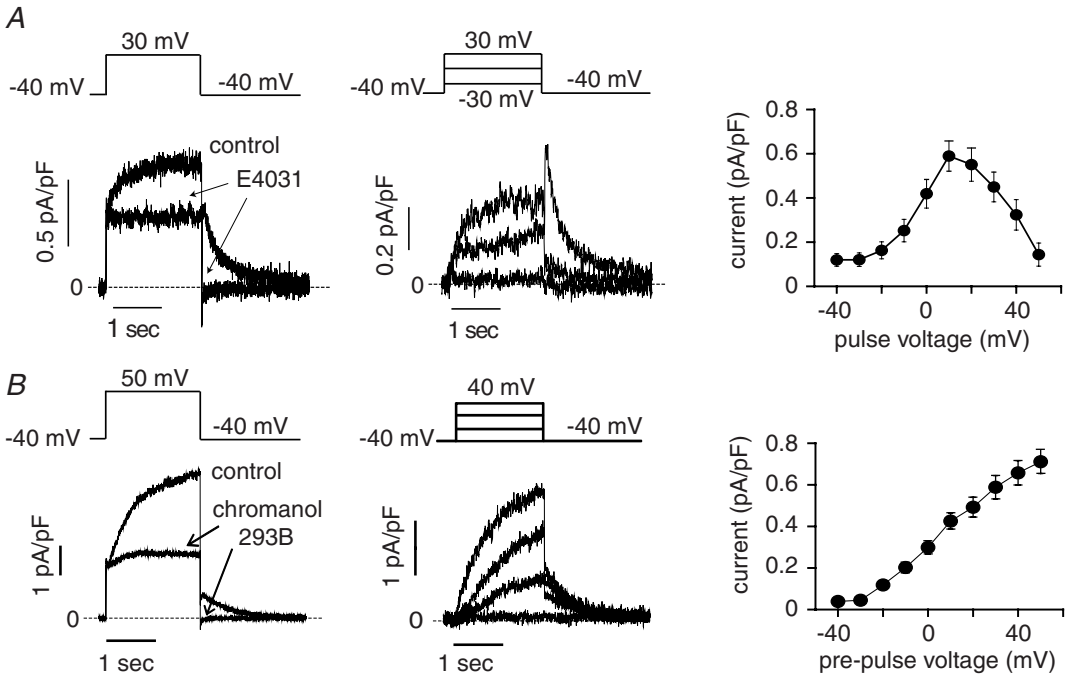

Figure 2. Pharmacological dissection of two delayed rectifier K^+ channels in hESC derived myocytes
A, left panel, in the presence of chromanol 293B (30 μmol l^{-1}) in the recording solution (control), E4031 (5 μmol l^{-1}) inhibits the rapidly activating current at 30 mV (2 s test pulse from holding potential (HP) of −40 mV) and blocks its corresponding tail current at −40 mV (arrows in left panel). Dashed line indicates zero current. Middle panel, representative E4031-sensitive current traces recorded at different test pulses (2 s test pulses to: −30, 0 and 30 mV; HP −40 mV; 0.1 Hz). Dashed line is zero current. Right panel, current–voltage relationship established by measuring the E4031-sensitive current in the end of 2 s depolarizing test pulses from −40 to 50 mV. *B*, left panel, in the presence of E4031 (5 μmol l^{-1}) in the recording solution (control), chromanol 293B (30 μmol l^{-1}) inhibits the slowly activating current at 50 mV (2 s test pulse from HP of −40 mV) and blocks its corresponding tail current at −40 mV (arrows in left panel). Dashed line indicates zero current. Middle panel, representative chromanol-sensitive current traces recorded at different test pulses (2 s test pulses to: −40, 0, 20 and 40 mV; HP −40 mV; 0.1 Hz). Dashed line is zero current. Right panel, current–voltage relationship established from the chromanol-sensitive maximum tail current measured during the repolarizing pulse at −40 mV that follows 2 s depolarizing test pulses from −40 to 50 mV. Data are shown as means ± SEM.

CTX-sensitive channels were then transiently expressed in hESC-CMs with (1:1 ratio) or without KCNE1 and CTX (70 nmol l^{-1}) was used to isolate the recombinant channels from the endogenous I_{Ks} channels (Fig. 4). As shown in Fig. 4*E*, robust expression of CTX-sensitive channels is observed in hESC-CMs with tail currents ~10-fold larger than endogenous I_{Ks}. Also, the voltage dependence of activation of CTX-sensitive channels was similar to that measured in HEK293 cells (CTX-KCNQ1: $V_{1/2} = -27.2 \pm 4.5$ mV, $n = 4$; CTX-KCNQ1/KCNE1: $V_{1/2} = 31.8 \pm 1.3$ mV, $n = 5$; N.S. compared to corresponding channels in HEK293 cells) (Fig. 4*F*). These results further indicate that the voltage dependence of activation of endogenous hESC-CMs I_{Ks} lies between KCNQ1 alone and KCNQ1/KCNE1 heteromultimers in the same cell type. This result suggests that either KCNE1 is expressed at low level in hESC-CMs and/or that other KCNE subunits assemble KCNQ1 therefore changing the properties of the whole I_{Ks} current.

Overexpression of recombinant KCNE1 in hESC-CMs shifts $V_{1/2}$ of endogenous I_{Ks} channels

To test whether further KCNE1 could modulate the channel, we over-expressed KCNE1 alone in hESC-CMs and compared the biophysical properties to that of endogenous I_{Ks} channels. I_{Ks} in KCNE1-transfected cells was still abolished by 30 μmol l^{-1} chromanol 293B (Fig. 5*A*) and activated more slowly (at 10 mV, $t_{1/2} = 973 \pm 32$ ms, $n = 4$) than in non-transfected cells ($t_{1/2} = 859 \pm 23$ ms, $n = 11$, $P < 0.05$) (Fig. 5*B*). The mid-point of activation of I_{Ks} in KCNE1-transfected cells was shifted to more positive voltages (from $V_{1/2} = 9.1 \pm 1.7$ mV, $n = 11$, in non-transfected cells to $V_{1/2} = 33.6 \pm 1.4$ mV, $n = 4$, in KCNE1-transfected cells, $P < 0.001$) (Fig. 5*D*) and was not significantly different from CTX-KCNQ1 channels co-expressed with KCNE1 (Fig. 4*F*). Despite the shift in activation, which would suggest a smaller open probability for the channel at any given voltage, I_{Ks} maximum tail current density at +50 mV was significantly larger in

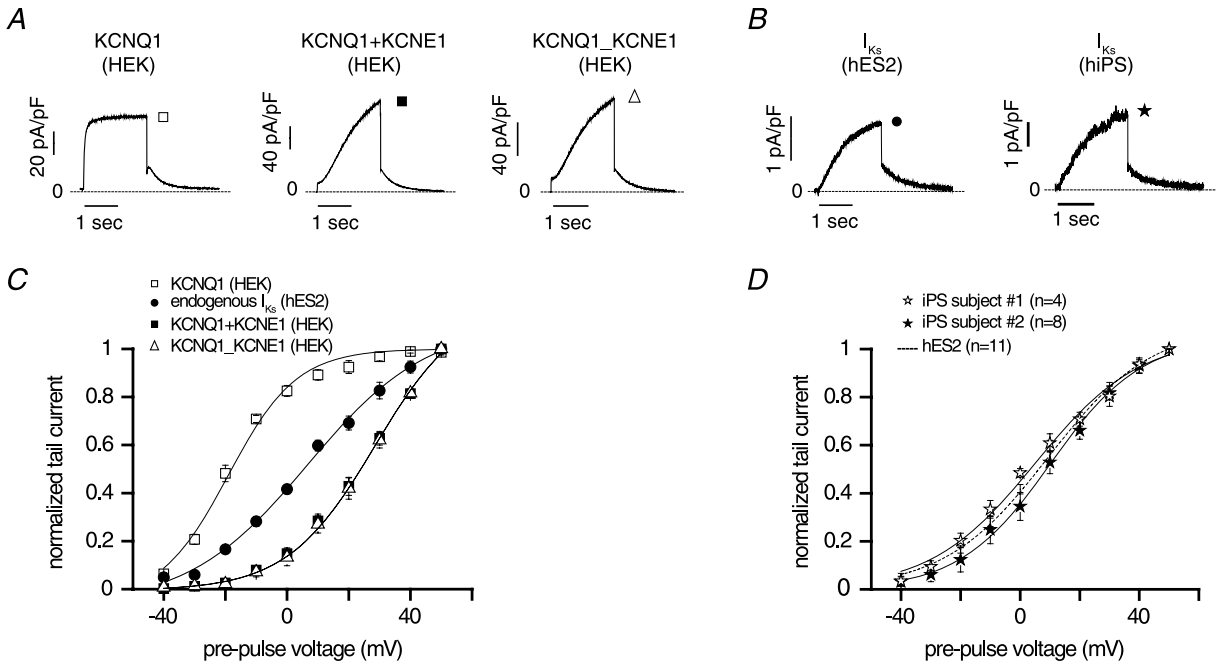

Figure 3. Current traces recorded during 2 s test pulse to 40 mV (HP = −40 mV) followed by repolarizing pulse to −40 mV
A, HEK293 (HEK) cells were transfected with the following recombinant channels: KCNQ1 (left panel, average of 4 cells); KCNQ1+KCNE1 (middle panel, average of 9 cells); KCNQ1_KCNE1 tandem multimer (right panel, average of 7 cells). Dashed line indicates zero current. *B*, endogenous I_{Ks} current was recorded in cardiac myocytes derived from hES2 cells (left panel) and from hiPSCs cells (right panel). Dashed line indicates zero current. *C*, normalized tail currents measured at −40 mV *vs.* pre-pulse voltage for recombinant channels (KCNQ1, open squares, $n = 4$; KCNQ1+KCNE1, filled squares, $n = 9$; KCNQ1_KCNE1 tandem multimer, open triangles, $n = 7$) expressed in HEK293 cells and endogenous I_{Ks} channels recorded in cardiac myocytes derived from hES2 cells (filled circles, $n = 11$). Data are shown as means ± SEM. *D*, normalized tail currents measured at −40 mV *vs.* pre-pulse voltage for endogenous I_{Ks} channels recorded in cardiac cells derived from human induced pluripotent stem (iPS) cells (iPS cells from subject no. 1, open stars, $n = 4$; iPS cells from subject no. 2, filled stars, $n = 8$). Dashed line represents activation curve for endogenous I_{Ks} channels in hES2 cells ($n = 11$). Data are shown as means ± SEM.

KCNE1-transfected cells: 1.41 ± 0.36 pA pF^{-1} ($n = 4$) *vs.* 0.71 ± 0.05 pA pF^{-1} ($n = 11$, $P < 0.001$) (Fig. 5*C*). These characteristics, slowing of activation kinetics, increased tail current and depolarized shift in activation are hallmarks of KCNE1 modulation of KCNQ1, suggesting endogenous I_{Ks} channels in hESC-CMs can be further regulated by KCNE1.

Figure 6 summarizes data and compares measured $V_{1/2}$ values for all constructs and cells studied. The figure clearly shows that I_{Ks} channel activity in hESC-CMs and hiPSC-CMS can be readily distinguished from KCNQ1 homomeric channels and that the activation voltages measured in the hiPSC-CMs and in the hESC-CMs are not significantly different from each other, but in both cases the measured $V_{1/2}$ values are significantly different from $V_{1/2}$ values obtained from expression of KCNQ1_KCNE1 tandem multimer with a fixed KCNQ1/KCNE1 1:1 stoichiometry and from independent co-expression of KCNQ1 and KCNE1. Importantly hESC-CM transfection with additional KCNE1 subunits rescues $V_{1/2}$ of KCNQ1/KCNE1 channels with a 1:1 stoichiometry.

Discussion

In this study, we report for the first time, a systematic investigation of the biophysical properties of I_{Ks} channels expressed in hESC-CMs and demonstrate that these cells can be used as a platform to express and study recombinant ion channels. Also, we find that the functional properties of endogenous I_{Ks} channels expressed in hESC-CMs and in hiPSC-CMs are similar and that they are consistent with KCNQ1/KCNE1 heteromultimers. However, the properties of the expressed channels are consistent with less than maximal KCNE1 to KCNQ1 ratios (stoichiometry). Co-expression of additional KCNE1 shows a marked effect on the function of expressed channels suggesting a pathway for I_{Ks} channel modulation that might occur in the developing heart or in human disease.

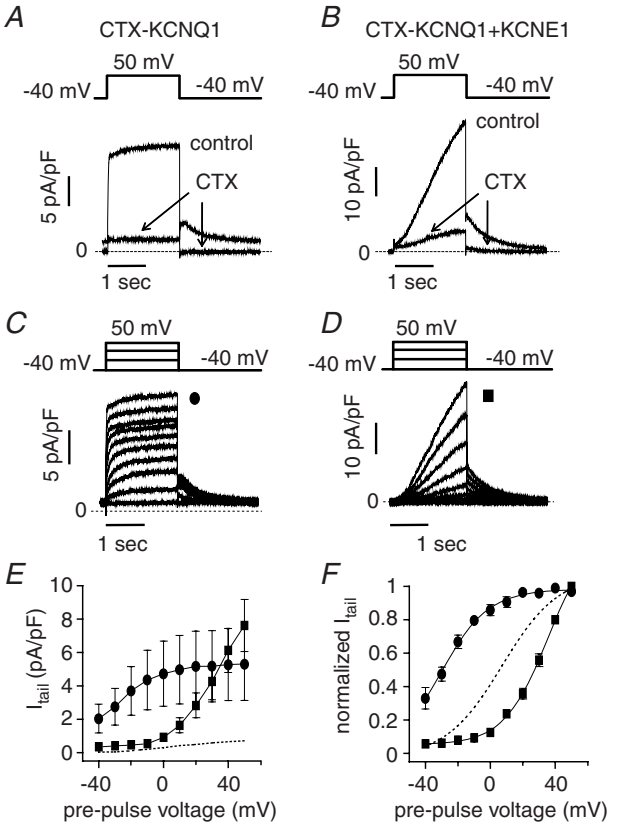

Figure 4. Biophysical properties of recombinant CTX-sensitive I_{Ks} channels expressed in hESC-CMs
A and *B*, CTX (70 nmol l^{-1}, arrows) inhibits CTX-KCNQ1 (*A*) and CTX-KCNQ1+KCNE1 (*B*) currents at 50 mV (2 s test pulse from holding potential of −40 mV) and blocks the corresponding tail currents at −40 mV. Dashed line indicates zero current. *C* and *D*, representative CTX-sensitive current traces recorded at different test pulses (2 s test pulses from −40 to 50 mV; HP −40 mV; 0.1 Hz). Dashed line is zero current. Average ($n = 5$) tail current (*E*) and normalized tail current (*F*) measured at −40 mV *vs.* test pulse voltage for CTX-KCNQ1 (circles) and CTX-KCNQ1+KCNE1 (squares). Dashed line indicates the level of current for endogenous I_{Ks}. Data are shown as means ± SEM.

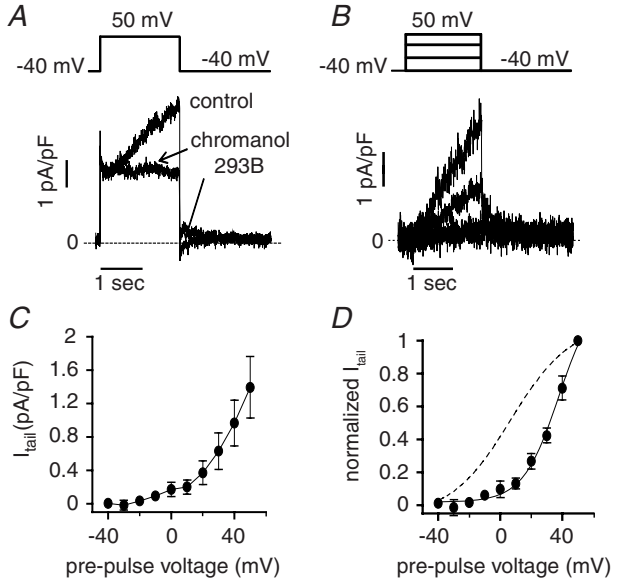

Figure 5. Biophysical properties of endogenous I_{Ks} in hESC-CMs transfected with KCNE1
A, chromanol 293B (30 μmol l^{-1}, arrows) inhibits the slowly activating current at 50 mV (2 s test pulse from holding potential of −40 mV) and blocks its corresponding tail current at −40 mV. Dashed line indicates zero current. *B*, representative chromanol-sensitive current traces recorded at different test pulses (2 s test pulses to: −40, 0, 30 and 50 mV; HP −40 mV; 0.1 Hz). Dashed line is zero current. Average ($n = 4$) I_{Ks} tail current (*C*) and normalized tail current (*D*) measured at −40 mV *vs.* test pulse voltage. Dashed line indicates activation curve for I_{Ks} in non-transfected hESC-CMs. Data are shown as means ± SEM.

Whole cell patch clamp recordings demonstrate a large, slowly activating current with sensitivity to chromanol 293B, clearly demonstrating the presence of I_{Ks} channels in hESC-CMs. This finding is consistent with recently published reports in hESC-CMs suggesting the presence of I_{Ks} (Otsuji *et al.* 2010) and showing prolongation of APD by the I_{Ks} blocker chromanol 293B (Peng *et al.* 2010). Furthermore, we provide the first detailed characterization of the biophysical properties of I_{Ks} in hESC-CMs. The properties of I_{Ks} we report in hESC-CMs are very similar to those observed in human adult ventricular myocytes with half-maximal activation voltage of +12 mV (Li *et al.* 1996). Using over-expression of KCNQ1 and KCNE1, we were able to explore the properties of endogenous I_{Ks} in relation to recombinant channels. By engineering a CTX sensitivity into KCNQ1, over-expressed channels could be isolated from endogenous channels. Interestingly, we found the endogenous channel activity to be intermediate to KCNQ1 and KCNQ1/KCNE1 both in classic heterologous systems (HEK293) as well as in hESC-CMs. Specifically, we find that endogenous I_{Ks} channels in hESC-CMs activate at voltages between that of homomeric KCNQ1 channels and heteromeric KCNQ1/KCNE1 channels (Fig. 4). As the sequence of KCNQ1 and KCNE1 were genotyped as normal, genetic variation does not play a role in this discrepancy. Further qPCR shows KCNE1 as the primary KNCE family member in these cells and the presence of small amount of KCNE4 would only adjust the magnitude and not the biophysical properties of the channel. Altogether, these data strongly suggest that KCNE1 is the main KCNE subunit assembling with KCNQ1 in the I_{Ks} channels we detect in hESC-CMs, and that not all channels are assembled in a 1:1 stoichiometry. This was confirmed by experiments in which we used transient transfection to increase KCNE1 expression in hESC-CMs (Fig. 5). We found that endogenous I_{Ks} in transfected cells was larger than in non-transfected cells, that the current's onset of activation was slower and that channels mid-point of activation was remarkably shifted to the right and reached that of KCNQ1/KCNE1 heteromultimers (Fig. 6).

Differing studies in the literature have suggested either that I_{Ks} channels may be composed of KCNQ1/KCNE1 complexes with variable stoichiometries (Wang *et al.* 1998; Nakajo *et al.* 2010; Osteen *et al.* 2010) or have a fixed stoichiometry, with KCNQ1 co-assembling with KCNE1 in a 4:2 stoichiometry (Chen *et al.* 2003; Morin & Kobertz, 2008). If a fixed stoichiometry is assumed, the mid-point of activation of endogenous I_{Ks} can only be achieved by a mixed population composed of KCNQ1/KCNE1 channels in a 4:2 stoichiometry combined with KCNQ1 channels alone. To test whether a linear combination

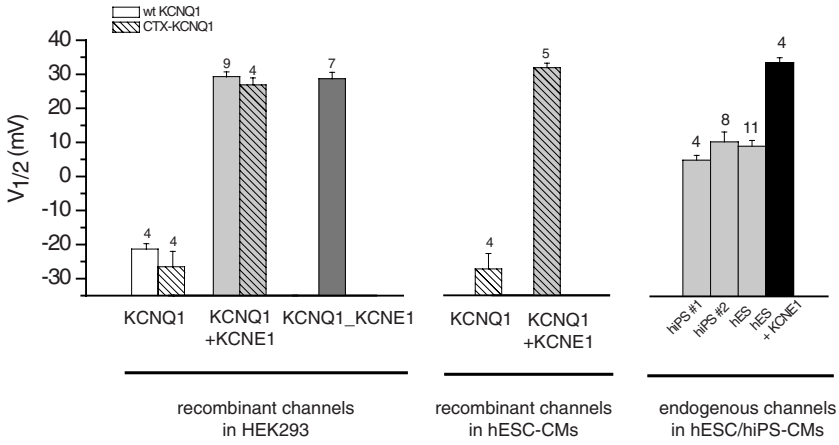

Figure 6. Bar graph summaries comparing the mid-point of activation ($V_{1/2}$) of endogenous I_{Ks} channels in cardiac cells derived from human stem cells (hESC-CMs and hiPSC-CMs, right panel) with those of recombinant channels expressed in HEK293 cells (left panel) and in hESC-CMs (middle panel)
$V_{1/2}$ measurements for endogenous I_{Ks} channels were the same for myocytes differentiated from hESCs and from hiPSCs but significantly different from KCNQ1 alone ($P < 0.001$) and all other combinations of KCNQ1/KCNE1 ($P < 0.001$). Left panel, HEK293 cells were transfected with either WT KCNQ1 (open boxes) or CTX-KCNQ1 (hatched boxes) in the absence (white boxes) or presence (grey boxes) of KCNE1. In the latter condition, ratios of KCNE1/KCNQ1 cDNA were 1. 'KCNQ1_KCNE1' corresponds to tandem multimer channels in which KCNQ1/KCNE1 stoichiometry is fixed at a 1:1 ratio. Middle panel, $V_{1/2}$ measurements of CTX-sensitive recombinant channels transfected in hESC-CMs. Right panel, The mid-point of activation of endogenous I_{Ks} channels in hESC-CMs and in two different lines of hiPSC-CMs (hiPS no. 1, hiPS no. 2) is similar and falls in between that of homomeric KCNQ1 channels and of heteromeric KCNQ1/KCNE1 channels expressed in HEK293 cells and in hESC-CMs. In hESC-CMs transfected with KCNE1 subunits ('hES+KCNE1', black box), $V_{1/2}$ measurement for endogenous I_{Ks} is more positive than in non-transfected cells ($P < 0.001$) but is not significantly different from that of heteromeric KCNQ1/KCNE1 channels and of tandem multimer channels ('KCNQ1_KCNE1') in which KCNQ1/KCNE1 stoichiometry is fixed at a 1:1 ratio.

of channels with and without KCNE1 can reproduce our experimental findings, computational models were employed. Figure 7 shows the predicted results of KCNQ1 channels alone (Seebohm *et al.* 2003), KCNQ1+KCNE1 channels (simulating KCNE1 overexpression; Imredy *et al.* 2008), and a mixed population of the two (at a ratio that reproduces the observed half-maximal activation voltage in endogenous I_{Ks}). With these assumptions, the predicted response of the mixed population diverges substantially from the behaviour observed experimentally. First, the simulated step current is bi-exponential with a prominent initial fast component that shows no delayed sigmoidal activation. Secondly, the predicted *I–V* relation is discordant from experiment, with a voltage dependence that is much more graded. Lastly, due to the differences in single channel conductance, the simulations imply nearly 80% of the channels co-assemble without KCNE1. These results favour the alternative hypothesis that endogenous hESC-CM I_{Ks} is a co-assembled channel at stoichiometry less than 1:1. Our results are also consistent with endogenous I_{Ks} channels that could be further regulated by alterations in KCNE1 expression either in development toward a specific cardiac ventricular cell type or in disease (Radicke *et al.* 2006; Watanabe *et al.* 2007; Soltysinska *et al.* 2009).

Most of our current knowledge of the cardiac I_{Ks} channel complex and its pathological role has been obtained from studies using heterologous expression systems (Charpentier *et al.* 2010; Lu & Kass, 2010) and genetically altered mice (Marx *et al.* 2002) and rabbits (Brunner *et al.* 2008). However, a new cellular model in which the functional consequences of inherited mutations of the channel can be studied in the context of a human cardiac environment is still needed to address many important questions regarding the mechanistic basis of heritable arrhythmia and to explore potential patient-specific treatment. The results of this study demonstrate the fidelity of hESC-CMs as a platform for assaying the biophysical properties of the I_{Ks} channel's native and mutant gene products in a human CM. Consequently, hESC-CMs may serve as a baseline for studies of heritable arrhythmia caused by mutation in I_{Ks} associated genes KCNQ1 (LQT-1, FAF), KCNE1 (LQT-5), and AKAP9 (LQT-11).

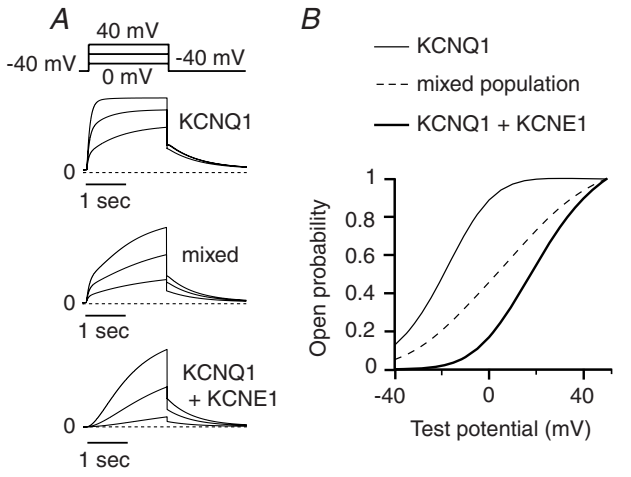

Figure 7. Computer-generated models suggest distinction between monomeric KCNQ1, endogenous I_{Ks} and I_{Ks} with KCNE1 overexpression
A, model-derived current traces for KCNQ1 monomeric channels, a linear combination (~80%–20%) of KCNQ1 and KCNQ1+KCNE1 channels (simulating endogenous hESC-CMs I_{Ks} voltage dependence), and KCNQ1+KCNE1 channels alone. *B*, activation curves taken from maximal open probability for test voltages from −40 to +50 mV show that a population of channels composed of KCNQ1 homomers mixed with KCNQ1/KCNE1 heteromultimers would predict a substantially flatter activation curve.

References

Barhanin J, Lesage F, Guillemare E, Fink M, Lazdunski M & Romey G (1996). K_VLQT1 and lsK (minK) proteins associate to form the I_{Ks} cardiac potassium current. *Nature* **384**, 78–80.

Brunner M, Peng X, Liu GX, Ren XQ, Ziv O, Choi BR, Mathur R, Hajjiri M, Odening KE, Steinberg E, Folco EJ, Pringa E, Centracchio J, Macharzina RR, Donahay T, Schofield L, Rana N, Kirk M, Mitchell GF, Poppas A, Zehender M & Koren G (2008). Mechanisms of cardiac arrhythmias and sudden death in transgenic rabbits with long QT syndrome. *J Clin Invest* **118**, 2246–2259.

Busch AE, Suessbrich H, Waldegger S, Sailer E, Greger R, Lang H, Lang F, Gibson KJ & Maylie JG (1996). Inhibition of IKs in guinea pig cardiac myocytes and guinea pig IsK channels by the chromanol 293B. *Pflugers Arch* **432**, 1094–1096.

Charpentier F, Merot J, Loussouarn G & Baro I (2010). Delayed rectifier K^+ currents and cardiac repolarization. *J Mol Cell Cardiol* **48**, 37–44.

Chen H, Kim LA, Rajan S, Xu S & Goldstein SA (2003). Charybdotoxin binding in the I_{Ks} pore demonstrates two MinK subunits in each channel complex. *Neuron* **40**, 15–23.

Chung DY, Chan PJ, Bankston JR, Yang L, Liu G, Marx SO, Karlin A & Kass RS (2009). Location of KCNE1 relative to KCNQ1 in the I_{KS} potassium channel by disulfide cross-linking of substituted cysteines. *Proc Natl Acad Sci U S A* **106**, 743–748.

Fu JD, Jiang P, Rushing S, Liu J, Chiamvimonvat N & Li RA (2010). Na^+/Ca^{2+} exchanger is a determinant of excitation-contraction coupling in human embryonic stem cell-derived ventricular cardiomyocytes. *Stem Cells Dev* **19**, 773–782.

Grunnet M, Jespersen T, Rasmussen HB, Ljungstrom T, Jorgensen NK, Olesen SP & Klaerke DA (2002). KCNE4 is an inhibitory subunit to the KCNQ1 channel. *J Physiol* **542**, 119–130.

Imredy JP, Penniman JR, Dech SJ, Irving WD & Salata JJ (2008). Modeling of the adrenergic response of the human IKs current (hKCNQ1/hKCNE1) stably expressed in HEK-293 cells. *Am J Physiol Heart Circ Physiol* **295**, H1867–1881.

Kass RS & Wiegers SE (1982). The ionic basis of concentration-related effects of noradrenaline on the action potential of calf cardiac purkinje fibres. *J Physiol* **322**, 541–558.

Kennedy M, D'Souza SL, Lynch-Kattman M, Schwantz S & Keller G (2007). Development of the hemangioblast defines the onset of hematopoiesis in human ES cell differentiation cultures. *Blood* **109**, 2679–2687.

Li GR, Feng J, Yue L, Carrier M & Nattel S (1996). Evidence for two components of delayed rectifier K^+ current in human ventricular myocytes. *Circ Res* **78**, 689–696.

Lu JT & Kass RS (2010). Recent progress in congenital long QT syndrome. *Curr Opin Cardiol* **25**, 216–221.

Lundquist AL, Manderfield LJ, Vanoye CG, Rogers CS, Donahue BS, Chang PA, Drinkwater DC, Murray KT & George AL Jr (2005). Expression of multiple KCNE genes in human heart may enable variable modulation of I_{Ks}. *J Mol Cell Cardiol* **38**, 277–287.

Marx SO, Kurokawa J, Reiken S, Motoike H, D'Armiento J, Marks AR & Kass RS (2002). Requirement of a macromolecular signaling complex for β adrenergic receptor modulation of the KCNQ1-KCNE1 potassium channel. *Science* **295**, 496–499.

Moore JC, Fu J, Chan YC, Lin D, Tran H, Tse HF & Li RA (2008). Distinct cardiogenic preferences of two human embryonic stem cell (hESC) lines are imprinted in their proteomes in the pluripotent state. *Biochem Biophys Res Commun* **372**, 553–558.

Morin TJ & Kobertz WR (2008). Counting membrane-embedded KCNE β-subunits in functioning K^+ channel complexes. *Proc Natl Acad Sci U S A* **105**, 1478–1482.

Mummery C, Ward-van Oostwaard D, Doevendans P, Spijker R, van den Brink S, Hassink R, van der Heyden M, Opthof T, Pera M, de la Riviere AB, Passier R & Tertoolen L (2003). Differentiation of human embryonic stem cells to cardiomyocytes: role of coculture with visceral endoderm-like cells. *Circulation* **107**, 2733–2740.

Nakajo K, Ulbrich MH, Kubo Y & Isacoff EY (2010). Stoichiometry of the KCNQ1–KCNE1 ion channel complex. *Proc Natl Acad Sci U S A* **107**, 18862–18867.

Osteen JD, Sampson KJ & Kass RS (2010). The cardiac IKs channel, complex indeed. *Proc Natl Acad Sci U S A* **107**, 18751–18752.

Otsuji TG, Minami I, Kurose Y, Yamauchi K, Tada M & Nakatsuji N (2010). Progressive maturation in contracting cardiomyocytes derived from human embryonic stem cells: Qualitative effects on electrophysiological responses to drugs. *Stem Cell Res* **4**, 201–213.

Peng S, Lacerda AE, Kirsch GE, Brown AM & Bruening-Wright A (2010). The action potential and comparative pharmacology of stem cell-derived human cardiomyocytes. *J Pharmacol Toxicol Methods* **61**, 277–286.

Radicke S, Cotella D, Graf EM, Banse U, Jost N, Varro A, Tseng GN, Ravens U & Wettwer E (2006). Functional modulation of the transient outward current Ito by KCNE β-subunits and regional distribution in human non-failing and failing hearts. *Cardiovasc Res* **71**, 695–703.

Sampson KJ, Iyer V, Marks AR & Kass RS (2010). A computational model of Purkinje fibre single cell electrophysiology: implications for the long QT syndrome. *J Physiol* **588**, 2643–2655.

Sanguinetti MC, Curran ME, Zou A, Shen J, Spector PS, Atkinson DL & Keating MT (1996). Coassembly of K_VLQT1 and minK (IsK) proteins to form cardiac I(Ks) potassium channel. *Nature* **384**, 80–83.

Sanguinetti MC & Jurkiewicz NK (1990). Two components of cardiac delayed rectifier K^+ current. Differential sensitivity to block by class III antiarrhythmic agents. *J Gen Physiol* **96**, 195–215.

Schwake M, Jentsch TJ & Friedrich T (2003). A carboxy-terminal domain determines the subunit specificity of KCNQ K^+ channel assembly. *EMBO Rep* **4**, 76–81.

Seebohm G, Pusch M, Chen J & Sanguinetti MC (2003). Pharmacological activation of normal and arrhythmia-associated mutant KCNQ1 potassium channels. *Circ Res* **93**, 941–947.

Soltysinska E, Olesen S-P, Christ T, Wettwer E, Varró A, Grunnet M & Jespersen T (2009). Transmural expression of ion channels and transporters in human nondiseased and end-stage failing hearts. *Pflugers Arch* **459**, 11–23.

Somers A, Jean JC, Sommer CA, Omari A, Ford CC, Mills JA, Ying L, Sommer AG, Jean JM, Smith BW, Lafyatis R, Demierre MF, Weiss DJ, French DL, Gadue P, Murphy GJ, Mostoslavsky G & Kotton DN (2010). Generation of transgene-free lung disease-specific human induced pluripotent stem cells using a single excisable lentiviral stem cell cassette. *Stem Cells* **28**, 1728–1740.

Tellmann G (2006). LightCycler® 480 Real-Time PCR system: innovative solutions for relative quantification. *Biochemica* **4**, 16–17.

Terrenoire C, Clancy CE, Cormier JW, Sampson KJ & Kass RS (2005). Autonomic control of cardiac action potentials: role of potassium channel kinetics in response to sympathetic stimulation. *Circ Res* **96**, e25–34.

Tsai CT, Lai LP, Hwang JJ, Lin JL & Chiang FT (2008). Molecular genetics of atrial fibrillation. *J Am Coll Cardiol* **52**, 241–250.

Wang W, Xia J & Kass RS (1998). MinK-KvLQT1 fusion proteins, evidence for multiple stoichiometries of the assembled IsK channel. *J Biol Chem* **273**, 34069–34074.

Watanabe E, Yasui K, Kamiya K, Yamaguchi T, Sakuma I, Honjo H, Ozaki Y, Morimoto S, Hishida H & Kodama I (2007). Upregulation of KCNE1 induces QT interval prolongation in patients with chronic heart failure. *Circ J* **71**, 471–478.

Yang L, Soonpaa MH, Adler ED, Roepke TK, Kattman SJ, Kennedy M, Henckaerts E, Bonham K, Abbott GW, Linden RM, Field LJ & Keller GM (2008). Human cardiovascular progenitor cells develop from a KDR+ embryonic-stem-cell-derived population. *Nature* **453**, 524–528.

Yoshida Y & Yamanaka S (2010). Recent stem cell advances: induced pluripotent stem cells for disease modeling and stem cell-based regeneration. *Circulation* **122**, 80–87.

Author contributions

Conception and design of the experiments: K.W., C.T., K.J.S., G.K., D.N.K., K.S.K.; collection, analysis and interpretation of

data: K.W., C.T., K.J.S., V.I., J.D.O.; Drafting the article or revising it critically for important intellectual content: K.W., C.T., K.J.S., J.L., K.S.K. All authors approved the final version of the manuscript. Disclosures: none.

Acknowledgements

This work was supported by the following grants: NY State Stem Cell Program (NYSTEM) N09G125 (R.S.K.,G.K.); NY State Stem Cell Program (NYSTEM) N08T-034 (J.L.); NY Stem Cell Foundation CU10-0553 (K.W.): Abraham and Beatrice Spatz Trust (R.S.K.); NIH HL 44365-16 (R.S.K.).